Journal of Photochemistry and Photobiology A: Chemistry 281 (2014) 53–58

Contents lists available at ScienceDirect

Journal of Photochemistry and Photobiology A: Chemistry

journal homepage: www.elsevier.com/locate/jphotochem

In_2S_3 sensitized solar cells with a new passivation layer

Yaohong Zhang[a,b], Jun Zhu[a,*], Feng Liu[a], Guohua Wu[a], Junfeng Wei[a], Linhua Hu[a], Yang Huang[a], Changneng Zhang[a], Junwang Tang[c,***], Songyuan Dai[a,d,**]

[a] Key Lab of Novel Thin Film Solar Cells, Institute of Plasma Physics, Chinese Academy of Sciences, Hefei 230031, China
[b] Key Laboratory of Optoelectronic Materials Chemistry and Physics, Fujian Institute of Research on the Structure of Matter, Chinese Academy of Sciences, Fuzhou 350002, China
[c] Department of Chemical Engineering, University College of London, London WC1E 7JE, United Kingdom
[d] State Key Laboratory of Alternate Electrical Power System with Renewable Energy Sources, North China Electric Power University, Beijing 102206, China

ARTICLE INFO

Article history:
Received 30 October 2013
Received in revised form 11 February 2014
Accepted 27 February 2014
Available online 12 March 2014

Keywords:
Indium sulfide
Quantum dot
Solar cell
Passivation layer

ABSTRACT

In_2S_3 as a semiconductor sensitizer has the advantage of non-toxicity, good stability and high carrier mobility. In this paper, In_2S_3 sensitized solar cells were firstly prepared by a low cost chemical bath deposition methodology and then fully characterized by X-ray diffraction, scanning electron microscopy, transmission electron microscopy and X-ray photoelectron spectroscopy. The ZnS passivation layer modified the In_2S_3 sensitized TiO_2 photoanodes and resulted into enhanced J_{sc} and FF but a lowered V_{oc} compared with the original solar cell under AM1.5, 1 sun. More importantly, we have enhanced all FF, J_{sc} and V_{oc} when amorphous Y_2O_3 was used to passivate the In_2S_3 sensitized solar cells, achieving the highest FF of 65% among the reported similar solar cells.

1. Introduction

Dye-sensitized solar cells (DSCs) have been paid much attention in the past decades because of their low cost, relatively high efficiency and prosperous application future. The power conversion efficiency around 11.4% has been achieved using ruthenium complex as sensitizer together with I^-/I_3^- redox electrolyte of DSCs [1]. Porphyrin sensitized solar cells with $Co^{(II-III)}$ based redox electrolyte has reached 12.3% power conversion efficiency [2]. Very recently inorganic semiconductor quantum dots (QDs) which absorb light in the visible region, such as CdS [3,4], CdSe [5,6], InP [7], and Sb_2S_3 [8], have been used as sensitizers instead of organic dye in DSCs. QDs have strong absorption with high molar extinction coefficient than organic sensitizers. Further due to the quantum size effects, the absorption spectrum of QDs can be tuned by simply controlling the QDs' sizes or shapes. By using these unique advantages, the maximum theoretical power conversion efficiency of quantum dot sensitized solar cells (QDSSCs) is expected to be much higher than the DSCs [9], although the current benchmark work represents a very moderate efficiency.

In the majority of QDSSCs, the QD sensitizers employ toxic elements such as cadmium, lead, and arsenic, etc. [3,7,10] and there is a practical need to develop low toxic QD sensitizers. In_2S_3, a typical III–VI group sulfide, exists in three different structure forms: α-In_2S_3 (defect cubic structure), β-In_2S_3 (defect spinel structure) and γ-In_2S_3 (layered hexagonal structure). In fact, β-In_2S_3 is a well n-type photoactive semiconductor with a direct band gap about 2.0 eV, a relative large exciton Bohr radius approximately 34 nm [11–13] and a high carrier mobility [14]. Therefore β-In_2S_3 has been investigated as an inorganic semiconductor sensitizer in QDSSCs [15–17]. Arakawa et al. prepared In_2S_3 sensitized In_2O_3 solar cells with sulfidation of In_2O_3 thin film electrodes under H_2S atmosphere [15], while George et al. prepared In_2S_3 sensitized TiO_2 solar cells using atomic layer deposition with indium acetylacetonate ($In(acac)_3$) and H_2S as precursors [16]. In these efforts, the open circuit photovoltage V_{oc} is less than 0.3 V and the fill factor FF is less than 40%. Gan et al. reported the fabrication of a TiO_2–In_2S_3 core–shell nanorod array structure for QDSSCs and the In_2S_3 shell layer was prepared by using the low cost successive ionic layer adsorption and reaction (SILAR) method. However, the best FF (46%) of these devices is still low. Furthermore the reported V_{oc} is very modest as well therefore leading to a quite low energy conversion efficiency (much less than 1%) [17].

In order to enhance the solar energy conversion efficiency, the low V_{oc} and FF have to be increased which are mainly due to

* Corresponding author.
** Corresponding author at: State Key Laboratory of Alternate Electrical Power System with Renewable Energy Sources, North China Electric Power University, Beijing 102206, China. Tel.: +86 0551 65591377; fax: +86 0551 65591377.
*** Corresponding author. Tel.: +44 020 7679 7393; fax: +44 020 7383 2348.
E-mail addresses: zhujzhu@gmail.com (J. Zhu), junwang.tang@ucl.ac.uk (J. Tang), sydai@ipp.ac.cn (S. Dai).

http://dx.doi.org/10.1016/j.jphotochem.2014.02.012
1010-6030/

recombination of (i) electrons in TiO_2 and hole in β-In_2S_3 and (ii) electrons in TiO_2 and the oxidized electrolyte. The strategy used in the conventional DSCs to retard the recombination is to insert an insulation layer between TiO_2 and dye, such as Al_2O_3 layer [18]. In this paper, In_2S_3 sensitized solar cells were prepared by the robust and low cost chemical bath deposition (CBD) methodology. A ZnS passivated layer was inserted between the In_2S_3 sensitized TiO_2 photoanodes and the electrolyte. Based on these results, a further modified QDSSC, composing of amorphous Y_2O_3 shell passivated the In_2S_3 sensitized TiO_2 photoanodes was developed, which has not been reported previously. Interestingly, both cells represent very high V_{oc} and FF. More importantly, a 65% FF has been achieved on Y_2O_3 modified QDSSC, the highest value among similar QDSSCs and the V_{oc} achieved is also 73% higher than the very recent reports [15,16].

2. Experimental

2.1. Preparation of In_2S_3 sensitized TiO_2 photoanodes with passivation layers

The colloidal TiO_2 nanoparticles were prepared by hydrolysis of titanium tetraisopropoxide as described elsewhere [19,20]. The mesoporous TiO_2 photoanodes were obtained by screen printing TiO_2 paste on FTO glass (TEC-15, LOF), then sintering at 450 °C for 30 min in air. The TiO_2 film thickness was around 10 μm, which was determined by a profilometer (XP-2, AMBIOS Technology Inc., USA). For In_2S_3 deposition, the mesoporous TiO_2 photoanodes were immersed in a beaker containing a freshly prepared aqueous mixture of 0.05 M $InCl_3$ and 0.2 M thioacetamide. The beaker mouth was sealed with the Parafilm® M laboratory film, then maintained at 40 °C for 10 h in a thermostat water bath. After deposition, the mesoporous TiO_2 photoanodes were washed with water and dried in a vacuum drying chamber at room temperature. The ZnS passivation layer was prepared by SILAR process as described by Shen et al. and exhibited similar thickness [21,22]. The TiO_2/In_2S_3 film was coated with Y_2O_3 passivation layer by dipping the film in 0.1 M yttrium (III) acetate ethanol solution at room temperature for 30 min, followed by sintering at 400 °C for 5 min in Ar atmosphere.

2.2. QDSSC assembly

The platinized counter electrodes were prepared by spraying H_2PtCl_6 solution on FTO, followed by heating at 410 °C for 20 min [23]. The In_2S_3 sensitized TiO_2 photoanodes and Pt counter electrodes were assembled into a sandwich cell by heating with a 60 μm thermal adhesive film (Surlyn, DuPont). An I^-/I_3^- redox electrolyte solution of 0.05 M I_2, 0.1 M LiI, 0.6 M 1-propyl-2,3-dimethylimidazolium iodide (DMPII) in 3-methoxypropionitrile was filled from a hole made on the counter electrode, which was later sealed by thermal adhesive film and a cover glass. The active area of QDSSC was 0.5 cm × 0.5 cm = 0.25 cm^2 [24,25].

2.3. Characterization and measurements

The structure and crystallinity of the sample were investigated by X-ray diffraction (XRD, Rigaku, Japan). The composition and chemical state of $TiO_2/In_2S_3/Y_2O_3$ film was confirmed by X-ray photoelectron spectroscopy (XPS, Thermo Electron Corp., USA). Scanning electron microscopy (SEM) was used to examine the morphology of TiO_2/In_2S_3 film (Sirion200, FEI, Netherlands) and the transmission electron microscopy (TEM) was operated to observe the crystallinity and arrangement of TiO_2, In_2S_3 and Y_2O_3 (JEOL-2010, Japan). The absorbance of In_2S_3 sensitized TiO_2 film was recorded on a UV–vis spectrophotometer (U-3900H, Hitachi, Japan). The current density–voltage (J–V) characteristics of the QDSSCs were measured under AM 1.5 (100 mW/cm^2) illumination which was provided by a solar simulator (Oriel, USA), and recorded using a Keithley model 2420 digital source meter (Keithley, USA). Incident-photon-to-current efficiency (IPCE) curves were operated with a QE/IPCE measurement kit (Newport, USA) using a 300 W Xe lamp and a monochromator.

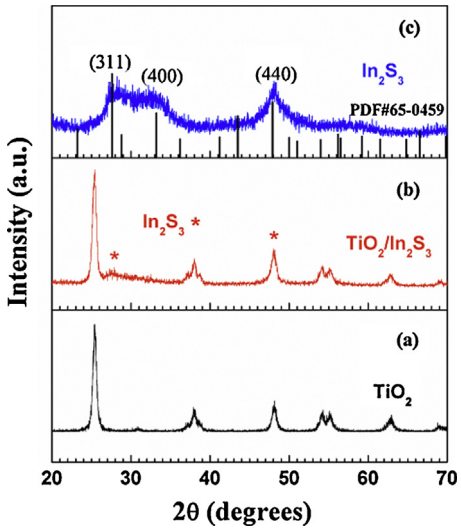

Fig. 1. XRD patterns of (a) pure TiO_2 nanoparticles, (b) TiO_2/In_2S_3 film and (c) pure In_2S_3 powder.

3. Results and discussion

3.1. Microstructure characterization of the In_2S_3 sensitized photoanodes

The powder X-ray diffraction (XRD) patterns of pure TiO_2 nanoparticles and In_2S_3 sensitized TiO_2 nanoparticles were shown in Fig. 1. It can be seen that the two samples show similar patterns except some small peaks in the sample of In_2S_3 sensitized TiO_2. In order to identify these small peaks, the pure In_2S_3 particles were prepared by the similar CBD method under the same condition. The XRD patterns of the single In_2S_3 particles were matched with that of cubic β-In_2S_3 (JCPDS#65-0459), indicating these weak peaks in the In_2S_3 sensitized TiO_2 belong to β-In_2S_3. Due to the relatively low quantity, only the most intense peak were observed and the peak width was large. The peaks at 2θ values of 27.6°, 33.2° and 47.8° are attributed to the (3 1 1), (4 0 0) and (4 4 0) planes of β-In_2S_3, respectively. The Y_2O_3 was not observed in the XRD patterns of Y_2O_3 coated TiO_2/In_2S_3 film, either due to high dispersed Y_2O_3 or amorphous phase.

The scanning electron microscopy (SEM) images of In_2S_3 sensitized TiO_2 mesoporous films were shown in Fig. 2. Obviously, although the porous structure of TiO_2 film was remained after the In_2S_3 deposition, the In_2S_3 coverage was relatively homogenous and a flake form of In_2S_3 was also exhibited. After the TiO_2/In_2S_3 film was coated with Y_2O_3 layer, there was an apparent change of surface morphology (Fig. 2b): the agglomeration and rearrangement of adjacent isolated In_2S_3 grains lead to surface smoothing of TiO_2/In_2S_3 films [26]. The significant morphology change was due to the annealing process at 400 °C for 5 min which is the last procedure during Y_2O_3 layer coating experiment. In fact, it will exhibit almost the same surface morphology as Fig. 2b if the TiO_2/In_2S_3 film is only annealed at 400 °C for 5 min without any extra coating procedure.

In order to get more information on the morphology of Y_2O_3, In_2S_3 sensitizer and their arrangement on TiO_2 surface, the TEM

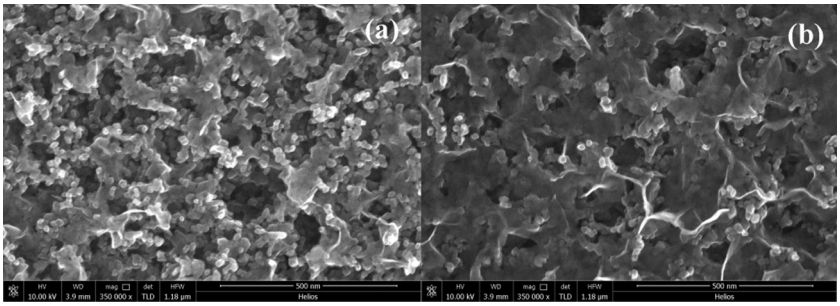

Fig. 2. SEM images of (a) as-deposited TiO_2/In_2S_3 film and (b) Y_2O_3 coated TiO_2/In_2S_3 film.

experiment was carried out. Fig. 3 shows the TEM image of In_2S_3 sensitized TiO_2 film by CBD and Fig. 4 shows the HR-TEM image. It can be seen that In_2S_3 is showing a nanosheet form on the TiO_2 film from the HR-TEM pattern, which is consistent with the results of the SEM images. The thickness and length of In_2S_3 were measured about 3 nm and 20 nm, respectively. The sizes of In_2S_3 are smaller than the Bohr radius (about 34 nm) [11–13], so they can be referred to as QDs. The observed spacing between the lattice planes was obtained as 2.70 Å for the (4 0 0) plane of β-In_2S_3. Around the TiO_2 nanoparticles and In_2S_3, a clear amorphous Y_2O_3 layer with a thickness of about 0.4 nm were observed and Y_2O_3 partially is

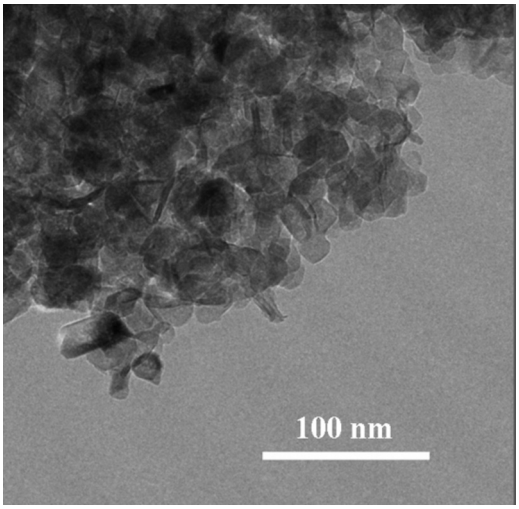

Fig. 3. TEM image of the Y_2O_3 coated TiO_2/In_2S_3 films.

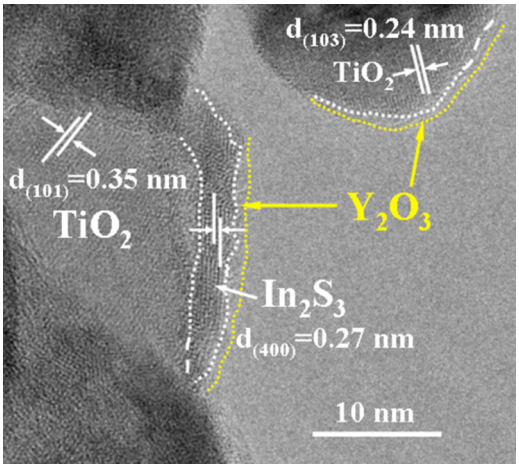

Fig. 4. HR-TEM image of the Y_2O_3 coated TiO_2/In_2S_3 film.

in direct contact with TiO_2. Because usually semiconductor sensitizers can not completely covered TiO_2 nanoparticles in QDSSCs prepared from both SILAR and presynthesis methods, the direct contact between Y_2O_3 and TiO_2 is as expected and similar with the case of ZnS passivation. We next investigated the impact of the thin amorphous Y_2O_3 shell on the In_2S_3 sensitized TiO_2 photoanode.

XPS characterization was taken to investigate the surface composition and the chemical state of the Y_2O_3 coated TiO_2/In_2S_3 film. The typical survey spectrum of the porous film was shown in Fig. 5, revealing the presence of In, S, Y, O and C elements. The peaks at 445.2 and 452.7 eV were, respectively, assigned to the binding energies of $In3d_{5/2}$ and $In3d_{3/2}$ of In_2S_3, while the peak at 161.3 and 162.5 eV could be attributed to the binding energy of $S2p_{3/2}$ and $S2p_{1/2}$ transition, respectively [27]. The observed binding energy values of In3d and S2p are identical to the reported data for In_2S_3 [17,28], suggesting that we obtain the stoichiometry of the In_2S_3 thin film, which is well consistent with the XRD results. The binding energies of $Y3d_{5/2}$ and $Y3d_{3/2}$ in the film were 158.2 and 160.1 eV, and higher than those ($Y3d_{5/2}$ 156.7, $Y3d_{3/2}$ 158.7) of the pure Y_2O_3 powder [29], indicating the Y—OH bond exists in the $TiO_2/In_2S_3/Y_2O_3$ film [30] due to the —OH groups adsorption on the amorphous Y_2O_3 surface [31]. The effect of surface chemical state on the interface detail such as interface dipole, energy barrier, et ac need further investigation, which could provide clues on the effect of inhibiting recombination. The peak of C may mainly be attributed to organic compounds pollution.

The light absorption of In_2S_3 sensitized TiO_2 films were shown in Fig. 6, indicating that the In_2S_3 have an apparent light absorption in the UV–vis region. Because the band gap of Y_2O_3 is so large (ca. 5.5 eV in bulk) [32], it has almost no contribution to light absorption and the band gap of TiO_2/In_2S_3 film. From Fig. 6b, the direct band gap of TiO_2/In_2S_3 film is about 2.8 eV, which is consistent with the literature [17], and is higher than the reported value of 2.0–2.3 eV for bulk β-In_2S_3 [33]. The band gap widening was attributed to the quantum size effect of In_2S_3.

3.2. The photovoltaic performance of the solar cells

The *J–V* characteristics of In_2S_3 sensitized solar cells without any passivation layer, with ZnS layer and with amorphous Y_2O_3 layer under illumination were shown in Fig. 7, and the related parameters of these cells were summarized in Table 1. Although the solar cell without any passivation layer based on chemical bath

Table 1
Photovoltaic performance parameters of the In_2S_3 sensitized solar cells.[a]

Photoanodes	V_{oc} (mV)	J_{sc} (mA/cm^2)	FF (%)	η (%)
TiO_2/In_2S_3	504 ± 5	0.42 ± 0.03	11 ± 3	0.02 ± 0.01
TiO_2/In_2S_3/ZnS	464 ± 3	0.88 ± 0.03	61 ± 2	0.25 ± 0.02
$TiO_2/In_2S_3/Y_2O_3$	524 ± 3	0.92 ± 0.02	65 ± 2	0.32 ± 0.02

[a] The listed results are average of four cells.

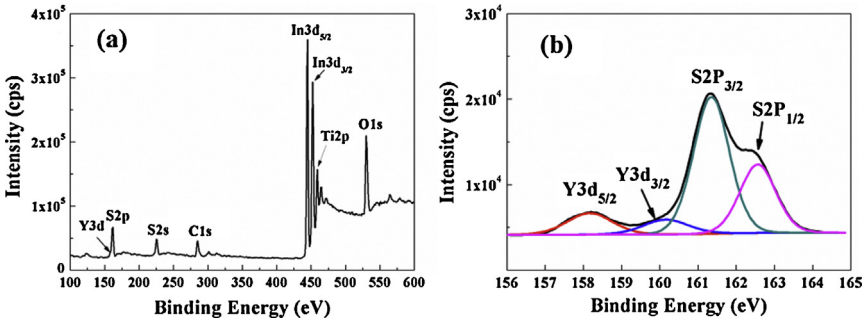

Fig. 5. XPS spectrums of Y_2O_3 coated TiO_2/In_2S_3 film: (a) survey spectrum, (b) binding energy spectrum of S2p and Y3d.

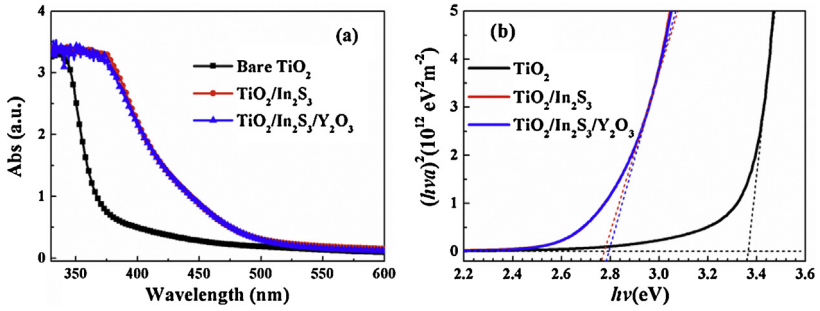

Fig. 6. UV–vis absorption (a) and Tauc plots (b) of TiO_2/In_2S_3 films.

deposition methodology gave an open circuit voltage 504 mV, almost double those of other methods [15,16], the FF is only 11%, resulting into the low power conversion efficiency of 0.02%. After the In_2S_3 sensitized TiO_2 photoanode was coated with ZnS passivation layer, there was a dramatic increase for the FF, from 11% to 61%, a high value for QDSSCs [34]. The significant improvement of the QDSSC performance after ZnS coating has been contributed to the reduced recombination between the electrons in TiO_2 and the electrolyte [35]. For the In_2S_3 sensitized solar cell without any passivation layer here, there must be a severe interface recombination because the unhomogeneous In_2S_3 deposition (Fig. 2a) leads to much surface area of TiO_2 nanoparticles exposed to the electrolyte. The severe recombination then leads to the low FF. After the ZnS coating, the TiO_2 surface states through which the recombination take place were passivated, then the high FF resulted.

Y_2O_3 coating TiO_2 before the dye adsorption process has been investigated in DSCs [36]. The Y_2O_3 coating forms an inherent energy barrier at the photoanode/electrolyte interface, by suppressing electron back transfer from electrode to the oxidized electrolyte to improve the V_{oc} and FF of DSCs. In addition, the Y_2O_3 coating can also increase the dye adsorption amount which is conductive to improve the J_{sc} of the solar cells [36]. However, there has not been report on employing Y_2O_3 coating in QDSSCs. Shalom et al. investigated the effect of amorphous TiO_2 coating on the performance of QDSSCs [37]. Therefore, the Y_2O_3 passivation layer was investigated. Thanks for the Y_2O_3 layer, the J_{sc} (0.92 mA/cm^2), the V_{oc} (524 mV) and the FF (65%) were achieved, highest among all solar cells investigated here. Moreover, to the best of our knowledge, the FF is the best value for the similar liquid QDSSCs up to now [16]. As a result, a relatively higher η (0.32%) was obtained for the $TiO_2/In_2S_3/Y_2O_3$ device, which was about 16-fold higher than the unmodified TiO_2/In_2S_3 device (0.02%). The IPCE of these In_2S_3 sensitized solar cells were also measured and shown in Fig. 8. The IPCE of the solar cell with passivation layer is much higher than the unmodified solar cell in the wavelength range of 350–500 nm. Y_2O_3 passivated solar cell gives higher IPCE than ZnS, in accordance with the J_{sc} trend.

The main effects of the amorphous Y_2O_3 layer in DSCs can be due to either the passivation of the surface states of TiO_2 or the forming of an energy barrier at the TiO_2/dye interface [36]. It is reasonable

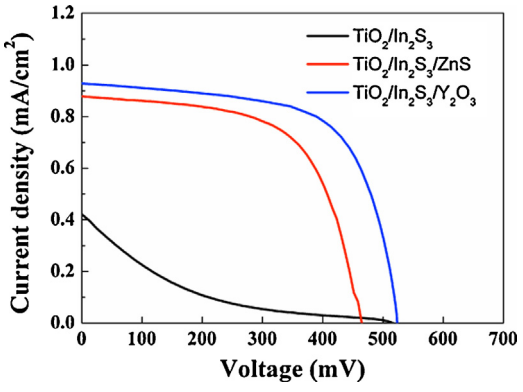

Fig. 7. *J–V* characteristics of In_2S_3 sensitized solar cells.

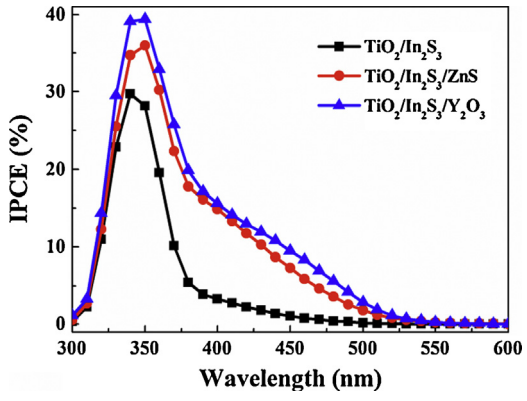

Fig. 8. The IPCE spectra of In_2S_3 sensitized solar cells.

Table 2
Photovoltaic performance parameters of the In_2S_3 sensitized TiO_2 solar cells based on different photoanodes.[a]

Photoanodes	V_{oc} (mV)	J_{sc} (mA/cm^2)	FF (%)	η (%)
TiO_2/In_2S_3	504 ± 5	0.42 ± 0.03	11 ± 3	0.02 ± 0.01
TiO_2/In_2S_3 (annealed)	362 ± 5	0.52 ± 0.03	39 ± 2	0.07 ± 0.01
$TiO_2/In_2S_3/Y_2O_3$	524 ± 3	0.92 ± 0.02	65 ± 2	0.32 ± 0.02
TiO_2/In_2S_3 (annealed)/Y_2O_3	557 ± 4	0.75 ± 0.02	66 ± 2	0.27 ± 0.02

[a] The listed results are average of four cells.

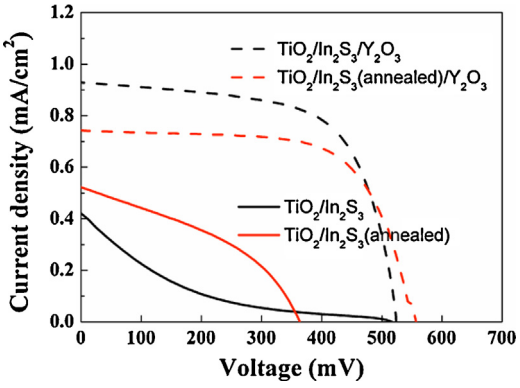

Fig. 9. The influence of annealing process on *J–V* characteristics of In_2S_3 sensitized TiO_2 solar cells.

to expect the same mechanism does work in In_2S_3 sensitized solar cells. However, because there was an annealing procedure during the Y_2O_3 layer coating experiment, we have carried out some experiments to elucidate the influence of the annealing process. It was found that only the annealing process without any other coating procedure will lead to the improvement of the device photovoltaic performance (Fig. 9). The J_{sc} increased from 0.42 mA/cm^2 to 0.52 mA/cm^2 and the FF increased from 11% to 39%, while the V_{oc} decreased from 504 mV to 362 mV and the overall power conversion efficiency increased from 0.02% to 0.07% (Table 2). However, for the device that combined the In_2S_3 annealing and the passivation layer coating process, TiO_2/In_2S_3 (annealed)/Y_2O_3 solar cell in Fig. 9, the power conversion efficiency (0.27%) is lower than that of the Y_2O_3 coated solar cell ($TiO_2/In_2S_3/Y_2O_3$ in Fig. 9) and the J_{sc} is lower too. The annealing treatment of TiO_2/In_2S_3 before Y_2O_3 coating could influence the surface states of In_2S_3 and therefore affect the adsorptive capacity of Y^{3+} cation, ultimately weaken the passivation of Y_2O_3 layer. The results indicated the Y_2O_3 passivation layer coating is the dominated factor that improves the device performance.

4. Conclusions

In_2S_3 sensitized solar cells were prepared by a low cost chemical bath deposition methodology. The ZnS layer coating the In_2S_3 sensitized TiO_2 photoanodes improved the fill factor and the short circuit current but lowered the V_{oc}. The amorphous Y_2O_3 shell was used to replace the ZnS layer and passivate the In_2S_3 sensitized TiO_2 photoanodes, which dramatically increased all the FF, V_{oc} and J_{sc}, achieving the highest FF of 65% and a V_{oc} close to the best reported. The further study is underway to improve the J_{sc} to achieve high energy conversion efficiency.

Conflict of interest

The authors declare no competing financial interest.

Acknowledgements

This work was supported by the National Basic Research Program of China under Grant No. 2011CBA00700, the National High Technology Research and Development Program of China under Grant No. 2011AA050527, the External Cooperation Program of the Chinese Academy of Sciences under Grant No. GJHZ1220, the Program of Hefei Center for Physical Science and Technology (2012FXZY006) and the National Natural Science Foundation of China under Grant Nos. 21173227, 21173228, 61204075.

References

[1] L. Han, A. Islam, H. Chen, C. Malapaka, B. Chiranjeevi, S. Zhang, X. Yang, M. Yanagida, High-efficiency dye-sensitized solar cell with a novel co-adsorbent, Energy & Environmental Science 5 (2012) 6057–6060.
[2] A. Yella, H.-W. Lee, H.N. Tsao, C. Yi, A.K. Chandiran, M.K. Nazeeruddin, E.W.-G. Diau, C.-Y. Yeh, S.M. Zakeeruddin, M. Grätzel, Porphyrin-sensitized solar cells with cobalt (II/III) – based redox electrolyte exceed 12 percent efficiency, Science 334 (2011) 629–634.
[3] S.-C. Lin, Y.-L. Lee, C.-H. Chang, Y.-J. Shen, Y.-M. Yang, Quantum-dot-sensitized solar cells: assembly of CdS-quantum-dots coupling techniques of self-assembled monolayer and chemical bath deposition, Applied Physics Letters 90 (2007) 143513–143517.
[4] G.S. Paul, J.H. Kim, M.-S. Kim, K. Do, J. Ko, J.-S. Yu, Different hierarchical nanostructured carbons as counter electrodes for CdS quantum dot solar cells, ACS Applied Materials & Interfaces 4 (2011) 375–381.
[5] H.J. Lee, J.-H. Yum, H.C. Leventis, S.M. Zakeeruddin, S.A. Haque, P. Chen, S.I. Seok, M. Grätzel, M.K. Nazeeruddin, CdSe quantum dot-sensitized solar cells exceeding efficiency 1% at full-sun intensity, The Journal of Physical Chemistry C 112 (2008) 11600–11608.
[6] Q. Shen, D. Arae, T. Toyoda, Photosensitization of nanostructured TiO_2 with CdSe quantum dots: effects of microstructure and electron transport in TiO_2 substrates, Journal of Photochemistry and Photobiology A: Chemistry 164 (2004) 75–80.
[7] A. Zaban, O.I. Mićić, B.A. Gregg, A.J. Nozik, Photosensitization of nanoporous TiO_2 electrodes with InP quantum dots, Langmuir 14 (1998) 3153–3156.
[8] S.-J. Moon, Y. Itzhaik, J.-H. Yum, S.M. Zakeeruddin, G. Hodes, M. Grätzel, Sb_2S_3-based mesoscopic solar cell using an organic hole conductor, The Journal of Physical Chemistry Letters 1 (2010) 1524–1527.
[9] A.J. Nozik, Quantum dot solar cells, low-dimensional systems and nanostructures, Physica E 14 (2002) 115–120.
[10] P. Yu, K. Zhu, A.G. Norman, S. Ferrere, A.J. Frank, A.J. Nozik, Nanocrystalline TiO_2 solar cells sensitized with InAs quantum dots, The Journal of Physical Chemistry B 110 (2006) 25451–25454.
[11] W.M. Qiu, M.S. Xu, X. Yang, F. Chen, Y.X. Nan, J.L. Zhang, H. Iwai, H.Z. Chen, Biomolecule-assisted hydrothermal synthesis of In_2S_3 porous films and enhanced photocatalytic properties, Journal of Materials Chemistry 21 (2011) 13327–13333.
[12] M.A. Franzman, R.L. Brutchey, Solution-phase synthesis of well-defined indium sulfide nanorods, Chemistry of Materials 21 (2009) 1790–1792.
[13] A. Datta, S.K. Panda, D. Ganguli, P. Mishra, S. Chaudhuri, In_2S_3 microporpous and their conversion to In_2O_3 nanobipyramids: simple synthesis approaches and characterization, Crystal Growth & Design 7 (2006) 163–169.
[14] W. Rehwald, G. Harbeke, On the conduction mechanism in single crystal β-indium sulfide In_2S_3, Journal of Physics and Chemistry of Solids 26 (1965) 1309–1324.
[15] K. Hara, K. Sayama, H. Arakawa, Semiconductor-sensitized solar cells based on nanocrystalline In_2S_3/In_2O_3 thin film electrodes, Solar Energy Materials and Solar Cells 62 (2000) 441–447.
[16] S.K. Sarkar, J.Y. Kim, D.N. Goldstein, N.R. Neale, K. Zhu, C.M. Elliott, A.J. Frank, S.M. George, In_2S_3 atomic layer deposition and its application as a sensitizer on TiO_2 nanotube arrays for solar energy conversion, The Journal of Physical Chemistry C 114 (2010) 8032–8039.
[17] X. Gan, X. Li, X. Gao, J. Qiu, F. Zhuge, TiO_2 nanorod arrays functionalized with In_2S_3 shell layer by a low-cost route for solar energy conversion, Nanotechnology 22 (2011) 305601.
[18] B.K.V. Ganapathy, S.-W. Rhee, Improved performance of dye-sensitized solar cells with TiO_2/alumina core–shell formation using atomic layer deposition, Journal of Power Sources 195 (2010) 5138–5143.

[19] L. Hu, S. Dai, J. Weng, S. Xiao, Y. Sui, Y. Huang, S. Chen, F. Kong, X. Pan, L. Liang, K. Wang, Microstructure design of nanoporous TiO_2 photoelectrodes for dye-sensitized solar cell modules, Journal of Physical Chemistry B 111 (2007) 358–362.
[20] J. Sheng, L. Hu, S. Xu, W. Liu, L. Mo, H. Tian, S. Dai, Characteristics of dye-sensitized solar cells based on the TiO_2 nanotube/nanoparticle composite electrodes, Journal of Materials Chemistry 21 (2011) 5457–5463.
[21] Q. Shen, J. Kobayashi, L.J. Diguna, T. Toyoda, Effect of ZnS coating on the photovoltaic properties of CdSe quantum dot-sensitized solar cells, Journal of Applied Physics 103 (2008) 084304.
[22] L.J. Diguna, Q. Shen, J. Kobayashi, T. Toyoda, High efficiency of CdSe quantum-dot-sensitized TiO_2 inverse opal solar cells, Applied Physics Letters 91 (2007) 023116.
[23] W. Liu, D. Kou, M. Cai, L. Hu, J. Sheng, H. Tian, N. Jiang, S. Dai, The intrinsic relation between the dynamic response and surface passivation in dye-sensitized solar cells based on different electrolytes, The Journal of Physical Chemistry C 114 (2010) 9965–9969.
[24] Y. Zhang, J. Zhu, X. Yu, J. Wei, L. Hu, S. Dai, The optical and electrochemical properties of CdS/CdSe co-sensitized TiO_2 solar cells prepared by successive ionic layer adsorption and reaction processes, Solar Energy 86 (2012) 964–971.
[25] X. Yu, J. Zhu, Y. Zhang, J. Weng, L. Hu, S. Dai, $SnSe_2$ quantum dot sensitized solar cells prepared employing molecular metal chalcogenide as precursors, Chemical Communications 48 (2012) 3324–3326.
[26] N. Revathi, P. Prathap, R.W. Miles, K.T.R. Reddy, Annealing effect on the physical properties of evaporated In_2S_3 films, Solar Energy Materials and Solar Cells 94 (2010) 1487–1491.
[27] S. Rengaraj, S. Venkataraj, C.W. Tai, Y. Kim, E. Repo, M. Sillanpaa, Self-assembled mesoporous hierarchical-like In_2S_3 hollow microspheres composed of nanofibers and nanosheets and their photocatalytic activity, Langmuir 27 (2011) 5534–5541.
[28] B. Chai, T.Y. Peng, P. Zeng, J. Mao, Synthesis of floriated In_2S_3 decorated with TiO(2) nanoparticles for efficient photocatalytic hydrogen production under visible light, Journal of Materials Chemistry 21 (2011) 14587–14593.
[29] W. Yao, Y. Guo, X. Liu, Y. Guo, Y. Wang, Y. Wang, Z. Zhang, G. Lu, Epoxidation of propylene by molecular oxygen over the $Ag–Y_2O_3–K_2O/a\text{-}Al_2O_3$ catalyst, Catalysis Letters 119 (2007) 185–190.
[30] M.D. Ulrich, J.E. Rowe, D. Niu, G.N. Parsons, Bonding and structure of ultrathin yttrium oxide films for Si field effect transistor gate dielectric applications, Journal of Vacuum Science & Technology B 21 (2003) 1792–1797.
[31] P. de Rouffignac, J.-S. Park, R.G. Gordon, Atomic layer deposition of Y_2O_3 thin films from yttrium tris(N,N′-diisopropylacetamidinate) and water, Chemistry of Materials 17 (2005) 4808–4814.
[32] Y.-N. Xu, Z.-q. Gu, W.Y. Ching, Electronic, structural, and optical properties of crystalline yttria, Physical Review B 56 (1997) 14993–15000.
[33] T. Asikainen, M. Ritala, M. Leskelä, Growth of In_2S_3 thin films by atomic layer epitaxy, Applied Surface Science 82/83 (1994) 122–125.
[34] Z. Yang, C.-Y. Chen, P. Roy, H.-T. Chang, Quantum dot-sensitized solar cells incorporating nanomaterials, Chemical Communications 47 (2011) 9561–9571.
[35] I. Mora-Sero, S. Gimenez, F. Fabregat-Santiago, R. Gomez, Q. Shen, T. Toyoda, J. Bisquert, Recombination in quantum dot sensitized solar cells, Accounts of Chemical Research 42 (2009) 1848–1857.
[36] A. Kay, M. Grätzel, Dye-sensitized core–shell nanocrystals: improved efficiency of mesoporous tin oxide electrodes coated with a thin layer of an insulating oxide, Chemistry of Materials 14 (2002) 2930–2935.
[37] M. Shalom, S. Dor, S. Rühle, L. Grinis, A. Zaban, Core/CdS quantum dot/shell mesoporous solar cells with improved stability and efficiency using an amorphous TiO_2 coating, The Journal of Physical Chemistry C 113 (2009) 3895–3898.